Lecture notes on topological insulators

Ming-Che Chang

Department of Physics, National Taiwan Normal University, Taipei, Taiwan

(Dated: December 23, 2020)

Contents

I. 2D TOPOLOGICAL INSULATOR

A. General theory

Analogous to the connection between 1D charge pump and 2D quantum Hall effect (see **??**), there is also a close connection between 1D spin pump and 2D topological insulator (TI). We can identify the parameter t with the Bloch momentum k_y of a 2D lattice system (see Fig. 1),

$$(k,t) \;\rightarrow\; (k_x,k_y). \tag{1.1}$$

The key ingredient that leads to the Z_2 values of ΔP_θ is the TRS of the 1D lattice at $t=0,T/2$. Because of the periodic variation, the edges of the domain at $t=T/2$ and $t=-T/2$ are related, just like the edges of a 2D BZ at $k_y=\pi$ and $-\pi$. Hence, $k_y=0,\pi$ play similar roles to $t=0,T/2$. Mathematically, one expects a similar Z_2 number from the following expression.

Consider time-reversal polarization P_θ along the x-direction. Define

$$\Delta P_\theta = P_\theta\left(k_y=\pi\right) - P_\theta\left(k_y=0\right). \tag{1.2}$$

It follows that (set $qa=1$)

$$\begin{aligned}
&(-1)^{\Delta P_\theta} \\
&= \prod_{n \text{ filled}} \frac{w_n(\Lambda_1)}{\sqrt{w_n^2(\Lambda_1)}}\frac{w_n(\Lambda_2)}{\sqrt{w_n^2(\Lambda_2)}}\frac{w_n(\Lambda_3)}{\sqrt{w_n^2(\Lambda_3)}}\frac{w_n(\Lambda_4)}{\sqrt{w_n^2(\Lambda_4)}} \\
&= \pm 1,
\end{aligned} \tag{1.3}$$

where Λ_i are the TRIM shown in Fig. 1.

We now consider the sewing matrix for N filled Kramer pairs. Since the Bloch states from different bands are orthogonal to each other, we have

$$\begin{aligned}
w_{m\alpha,n\beta}(\mathbf{k}) &= \langle u_{m-\mathbf{k}\alpha}|\Theta|u_{n\mathbf{k}\beta}\rangle &(1.4)\\
&= \delta_{mn} w_{n\alpha\beta}(\mathbf{k}). &(1.5)
\end{aligned}$$

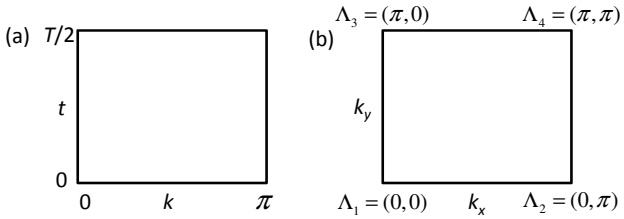

FIG. 1 (a) The domain of (k,t) variables in the 1D Fu-Kane model. (b) The first quadrant of the Brillouin zone in a 2D lattice model. The four corners are the TRIM.

It follows that,

$$\mathsf{w}(\mathbf{k}) = \begin{pmatrix} 0 & e^{i\chi_{1\mathbf{k}}} & 0 & 0 & 0 \\ -e^{i\chi_{1-\mathbf{k}}} & 0 & 0 & 0 & 0 \\ 0 & 0 & 0 & e^{i\chi_{2\mathbf{k}}} & 0 \\ 0 & 0 & -e^{i\chi_{2-\mathbf{k}}} & 0 & 0 \\ 0 & 0 & 0 & 0 & \ddots \end{pmatrix}. \tag{1.6}$$

One can show that its determinant at a TRIM is,

$$\det \mathsf{w}(\Lambda_i) = \prod_{n=1}^{N} w_n^2(\Lambda_i), \tag{1.7}$$

where $w_n(\mathbf{k}) = e^{i\chi_{n\mathbf{k}}}$.

For an *antisymmetric* $2N\times 2N$ matrix M, one can define its *pfaffian* (see wikipedia),

$$\text{pf } \mathsf{M} = \sum_P (-1)^P M_{i_1 j_1} M_{i_2 j_2}\cdots M_{i_N j_N}. \tag{1.8}$$

The subscripts,

$$(i_1,j_2),(i_2,j_2),\cdots,(i_N,j_N), \tag{1.9}$$

are all possible pairs from the string,

$$(1,2,3,\cdots,2N), \tag{1.10}$$

but under the constraints,

$$i_1<i_2<\cdots<i_N, \tag{1.11}$$

$$\text{and}\qquad i_1<j_1, i_2<j_2,\cdots,i_N<j_N. \tag{1.12}$$

P is a permutation from

$$(1,2,\ldots,2N)\rightarrow(i_1,j_1,\cdots,i_N,j_N), \tag{1.13}$$

and $(-1)^P$ is the sign of permutation p.

For example,

$$\text{pf}\begin{pmatrix} 0 & a \\ -a & 0 \end{pmatrix} = a, \tag{1.14}$$

$$\text{pf}\begin{pmatrix} 0 & a & b & c \\ -a & 0 & d & e \\ -b & -d & 0 & f \\ -c & -e & -f & 0 \end{pmatrix} = af - be + dc. \tag{1.15}$$

For the determinant in Eq. (1.7), we have

$$\text{pf } \mathsf{w}(\Lambda_i) = \prod_{n=1}^{N} w_n(\Lambda_i). \tag{1.16}$$

The square of Pfaffian pf M is the determinant $\det \mathsf{M}$,

$$\det \mathsf{M} = (\text{pf } \mathsf{M})^2. \tag{1.17}$$

Thus, pfaffian can be considered as the square root of determinant. If we define the a cumulative index for *filled* bands at *each* TRIM as,

$$\delta_i \equiv \prod_{n \text{ filled}} \frac{w_n(\Lambda_i)}{\sqrt{w_n^2(\Lambda_i)}} = \frac{\text{pf } \mathsf{w}(\Lambda_i)}{\sqrt{\det \mathsf{w}(\Lambda_i)}}, \tag{1.18}$$

then Eq. (1.3) can be written as (ΔP_θ is re-written as ν)

$$(-1)^\nu = \prod_{i=1}^{4} \frac{\text{pf } \mathsf{w}(\Lambda_i)}{\sqrt{\det \mathsf{w}(\Lambda_i)}} = \prod_{i=1}^{4} \delta_i. \tag{1.19}$$

An insulator with $\nu = 0$, 1 is called a trivial insulator and a topological insulator respectively.

1. Edge state in 2D topological insulator

If the 1D spin pump or the 2D lattice in Fig. 1 has an edge at certain cutoff x, then k (or k_x) is no longer a good quantum number. In Fig. **??**, we have shown the evolution of the edge states in a spin pump. By analogy, a 2D TI would have similar edge states inside the energy gap, crossing each other at TRIM (Fig. 2(b)).

In comparison, even though the edge states in a *trivial* insulator also need to cross each other at TRIM (Fig. 2(c)), the ways they link together are different. This is due to the fact that when $\delta_1\delta_2$ and $\delta_3\delta_4$ have opposite signs, $\nu = 1$, and we have a TI accompanied by a switch of Kramer-pair partner at TRIM. When $\delta_1\delta_2$ and $\delta_3\delta_4$ have the same sign, $\nu = 0$, and we have a trivial insulator with no switch of Kramer-pair partner.

If one plots a horizontal line (chemical potential) inside the energy gap, then it would cut the edge states in (b) odd number of times, but cut those in (c) even number of times. The former cannot be avoided by shifting or distorting the energy levels of edge states, while the latter can be avoided. Thus, the edge states in TI are robust, while those in trivial insulator are not.

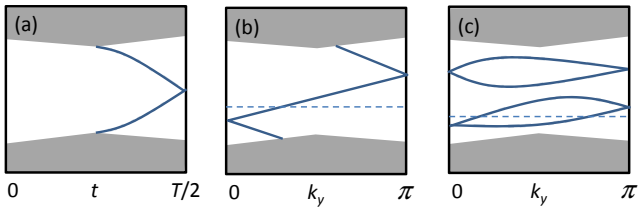

FIG. 2 Comparison of the edge states in (a) 1D spin pump, (b) 2D topological insulator, and (c) 2D trivial insulator. (a) is a schematic plot of the edge state in Fig. **??**. (b) and (c) show the energy levels in edge BZ.

2. Lattice with inversion symmetry

Even though ν is known to have two possible values, 0 and 1, it is not a trivial task to get explicit values of $\chi_{n\Lambda_i}$ at the first place. Fortunately, *if the lattice has space inversion symmetry* (SIS), then $w_n(\Lambda_i)/\sqrt{w_n^2(\Lambda_i)}$ is simply equal to the parity $\zeta_n(\Lambda_i)$ of the Bloch state $\psi_{n\Lambda_i\pm}$. Note that the parity of Kramer-pair states with index $\alpha = \pm$ is the same. This fact is proved below, following Nomura, 2013.

First, suppose Π is the SI operator, then

$$\begin{aligned} \psi_{n\mathbf{k}\alpha}(\mathbf{r}) \to \Pi\psi_{n\mathbf{k}\alpha}(\mathbf{r}) &\equiv \psi_{n\mathbf{k}\alpha}(-\mathbf{r}) \\ &= \psi_{n-\mathbf{k}\alpha}(\mathbf{r}), \end{aligned} \tag{1.20}$$

apart from a phase factor. The same is true for the cell-periodic state,

$$u_{n\mathbf{k}\alpha}(\mathbf{r}) \to \Pi u_{n\mathbf{k}\alpha}(\mathbf{r}) = u_{n-\mathbf{k}\alpha}(\mathbf{r}), \tag{1.21}$$

apart from a phase factor. If the lattice has SIS, then $\psi_{n\mathbf{k}\alpha}$ (but not $u_{n\mathbf{k}\alpha}$) are parity eigenstates at $\mathbf{k} = \Lambda_i$,

$$\Pi\psi_{n\Lambda_i\alpha}(\mathbf{r}) = \zeta_{n\Lambda_i}\psi_{n\Lambda_i\alpha}(\mathbf{r}). \tag{1.22}$$

The parity eigenvalue $\zeta_{n\Lambda_i} = 1$ or -1 is the same for the two Bloch states (with $\alpha = \pm$) in a Kramer pair.

Note that there is a slight difference between Bloch state $\psi_{n\mathbf{k}\alpha}$ and cell-periodic state $u_{n\mathbf{k}\alpha}$,

$$\psi_{n\mathbf{k}+\mathbf{G}\alpha} = \psi_{n\mathbf{k}\alpha}, \tag{1.23}$$

$$\text{but } u_{n\mathbf{k}+\mathbf{G}\alpha} = e^{-i\mathbf{G}\cdot\mathbf{r}}u_{n\mathbf{k}\alpha}. \tag{1.24}$$

Therefore, only the Bloch state can have $\psi_{n-\frac{\mathbf{G}}{2}\alpha} = \psi_{n\frac{\mathbf{G}}{2}\alpha}$.

Second, define a different type of sewing matrix as follows, for a particular Kramer pair with index n (suppressed here),

$$v_{\alpha\beta}(\mathbf{k}) \equiv \langle u_{\mathbf{k}\alpha}|\Pi\Theta|u_{\mathbf{k}\beta}\rangle. \tag{1.25}$$

(1) The matrix $v_{\alpha\beta}$ is anti-symmetric.
Pf: Using the relation $\langle\psi_1|\Theta|\psi_2\rangle = -\langle\Theta^2\psi_1|\Theta|\psi_2\rangle = -\langle\psi_2|\Theta\psi_1\rangle$, and $\Pi^\dagger = \Pi$, one has

$$v_{\alpha\beta} = \langle u_{\mathbf{k}\alpha}|\Pi\Theta|u_{\mathbf{k}\beta}\rangle \tag{1.26}$$

$$= \langle u_{\mathbf{k}\alpha}|\Theta\left(\Pi|u_{\mathbf{k}\beta}\rangle\right) \tag{1.27}$$

$$= -\langle u_{\mathbf{k}\beta}|\Pi\Theta|u_{\mathbf{k}\alpha}\rangle \tag{1.28}$$

$$= -v_{\beta\alpha}. \tag{1.29}$$

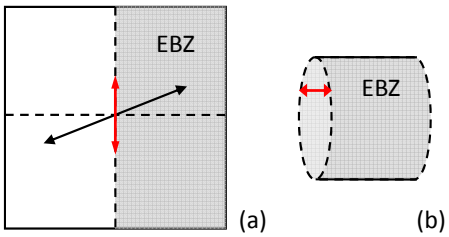

FIG. 3 (a) Time reversal conjugate pairs and effective Brillouin zone. (b) Folding the EBZ into a cylinder, with open edges.

(2) The matrix $v_{\alpha\beta}$ is unitary.
Pf: Using the relation $\langle\psi_1|\psi_2\rangle^* = \langle\psi_2|\psi_1\rangle$, one has

$$\begin{aligned}
\left(\mathsf{v}\mathsf{v}^\dagger\right)_{\alpha\gamma} &= \sum_\beta v_{\alpha\beta} v^*_{\gamma\beta} && (1.30)\\
&= \sum_\beta \langle u_{\mathbf{k}\alpha}|\Pi\Theta|u_{\mathbf{k}\beta}\rangle\langle u_{\mathbf{k}\gamma}|\Pi\Theta|u_{\mathbf{k}\beta}\rangle^* && (1.31)\\
&= \langle u_{\mathbf{k}\alpha}|u_{\mathbf{k}\gamma}\rangle && (1.32)\\
&= \delta_{\alpha\gamma}. && (1.33)
\end{aligned}$$

Similarly, one can also show that $\left(\mathsf{v}^\dagger\mathsf{v}\right)_{\alpha\gamma} = \delta_{\alpha\gamma}$. Therefore, it is unitary.

The matrix $w_{\alpha\beta}$ is also unitary, and is antisymmetric at Λ_i. Therefore, sewing matrices $w_{\alpha\beta}(\Lambda_i)$ and $v_{\alpha\beta}(\Lambda_i)$ differ by a multiplicative constant (the parity!) at TRIM:

$$\begin{aligned}
w_{\alpha\beta}(\Lambda_i) &= \langle u_{-\Lambda_i\alpha}|\Theta|u_{\Lambda_i\beta}\rangle && (1.34)\\
&= \langle \psi_{-\Lambda_i\alpha}|\Theta|\psi_{\Lambda_i\beta}\rangle && (1.35)\\
&= \langle \psi_{\Lambda_i\alpha}|\Pi^2\Theta|\psi_{\Lambda_i\beta}\rangle, \Pi^2 = 1 && (1.36)\\
&= \zeta_{\Lambda_i}\langle \psi_{\Lambda_i\alpha}|\Pi\Theta|\psi_{\Lambda_i\beta}\rangle && (1.37)\\
&= \zeta_{\Lambda_i}\langle u_{\Lambda_i\alpha}|\Pi\Theta|u_{\Lambda_i\beta}\rangle && (1.38)\\
&= \zeta_{\Lambda_i} v_{\alpha\beta}(\Lambda_i). && (1.39)
\end{aligned}$$

Under a gauge transformation,

$$\begin{aligned}
u_{k+} \to u'_{k+} &= e^{i\varphi_k} u_{k+}, && (1.40)\\
u_{k-} \to u'_{k-} &= u_{k-}, && (1.41)
\end{aligned}$$

the off-diagonal matrix element of $\mathsf{v}(\mathbf{k})$ transforms as,

$$v(\mathbf{k}) \to v'(\mathbf{k}) = e^{-i\varphi_k} v(\mathbf{k}). \quad (1.42)$$

Therefore, one can adjust its phase such that $v(\Lambda_i) = 1$. Hence,

$$w_n(\Lambda_i) = \zeta_n(\Lambda_i) v_n(\Lambda_i) = \zeta_n(\Lambda_i). \quad (1.43)$$

As a result,

$$\frac{w_n(\Lambda_i)}{\sqrt{w_n^2(\Lambda_i)}} = \zeta_n(\Lambda_i). \quad (1.44)$$

It follows that,

$$\delta_i = \prod_{n\in\text{filled}} \zeta_n(\Lambda_i), \quad (1.45)$$

which is the cumulative parity of filled Bloch states (pick only one $\zeta_n(\Lambda_i)$ for each Kramer pair) at a TRIM, and

$$(-1)^\nu = \prod_{i=1}^{4} \delta_i. \quad (1.46)$$

3. Z_2 integer ν as a topological invariant

• Chern number

To understand the Z_2 topology, we follow Moore and Balent's argument for 2D TI (Moore and Balents, 2007). Because of time-reversal symmetry, the degenerate Bloch states for $\mathbf{k}$ and $-\mathbf{k}$ in a Brillouin zone are time-reversal conjugate (see Fig. 3(a)). As their Berry curvatures cancel with each other, the first Chern number for a filled band vanishes. Since the domain of *independent* Bloch states cover only half of the BZ (called **effective Brillouin zone**, or EBZ), one may wonder if the integral of the Berry curvature over the EBZ could be quantized.

Unfortunately, since the EBZ does not form a closed surface (see Fig. 3(b)), no quantization is guaranteed. To fix this, one can put two caps with TR conjugation to close the EBZ. This closed surface should have an integer C_1, but its value depends on the caps of choice. Nevertheless, Moore and Balents proved that, because of the TR conjugation, the caps can only change C_1 by an even integer. That is, C_1 mod 2 is independent of the caps of choice. Therefore, C_1 mod 2 should be an intrinsic property of the EBZ itself. We thus have two topological classes: 0 being the usual insulator, and 1 being the topological insulator.

• Winding number

Fu and Kane showed that the Z_2 integer ν can be related to the winding number between two patches of gauge (Fu and Kane, 2006), which we now explain.

First, instead of Eq. (**??**) in Chap **??**, we adopt the TR-smooth gauge,

$$\begin{cases} \Theta\psi_{n\mathbf{k}+} = -\psi_{n-\mathbf{k}-}, \\ \Theta\psi_{n\mathbf{k}-} = +\psi_{n-\mathbf{k}+}. \end{cases} \quad (1.47)$$

As a result, the phases of Bloch states cannot be uniquely defined over the whole BZ. As in the case of the magnetic monopole in Chap **??**, we need to use more than one patch of gauge to get rid of singularity. This is the *topological obstruction* mentioned earlier.

Fig. 4 shows the EBZ covered by two patches of gauge. Along their boundary, the wave functions are connected by gauge transformation,

$$|u_{\mathbf{k}\alpha}\rangle_B = U_{\alpha\beta}|u_{\mathbf{k}\beta}\rangle_A, \quad (1.48)$$

where U is a U(2) matrix. Again we consider only one Kramer pair for simplicity.

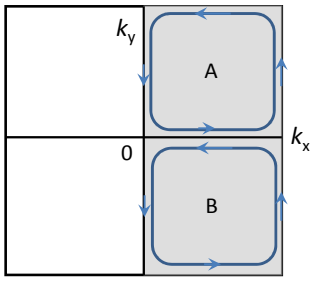

FIG. 4 Two patches of gauge in the EBZ.

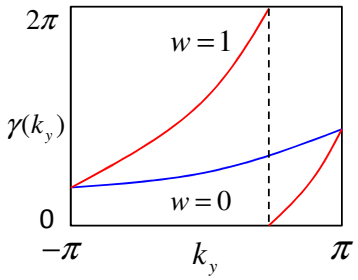

FIG. 5 Winding number of the Zak phase.

Recall that

$$\mathsf{A}_\ell^B = \mathsf{U}^\dagger \mathsf{A}_\ell^A \mathsf{U} + i\mathsf{U}^\dagger \frac{\partial}{\partial k_\ell}\mathsf{U}. \tag{1.49}$$

The topology of the Bloch states can be characterized by the winding number w of the U(1) phase of U around the closed loop ∂A in Fig. 4,

$$w = \frac{1}{2\pi i}\oint_{\partial A} d\mathbf{k}\cdot \mathrm{tr}\left(\mathsf{U}^\dagger \frac{\partial}{\partial \mathbf{k}}\mathsf{U}\right). \tag{1.50}$$

Taking the trace of Eq. (1.49), we have

$$w = \frac{1}{2\pi}\oint_{\partial A} d\mathbf{k}\cdot\left(\mathbf{A}^A - \mathbf{A}^B\right), \tag{1.51}$$

in which $\mathbf{A}^{A/B} \equiv \mathrm{tr}\ \vec{\mathsf{A}}^{A/B}$.

Since $|u^A_{\mathbf{k}\alpha}\rangle$ is smoothly defined inside A, one has

$$\oint_{\partial A} d\mathbf{k}\cdot\mathbf{A}^A = \int_A d^2k\ F_z^A. \tag{1.52}$$

The same cannot be done for $|u^B_{\mathbf{k}\alpha}\rangle$, since it is *not* smoothly defined in A. Instead, we write

$$\begin{aligned}\oint_{\partial A} d\mathbf{k}\cdot\mathbf{A}^B &= \oint_{\partial EBZ} d\mathbf{k}\cdot\mathbf{A}^B - \oint_{\partial B} d\mathbf{k}\cdot\mathbf{A}^B \\ &= \oint_{\partial EBZ} d\mathbf{k}\cdot\mathbf{A}^B - \int_B d^2k\ F_z^B \end{aligned} \tag{1.53}$$

Finally, combine Eqs. (1.52) with (1.53), we have (Fu and Kane, 2006),

$$w = \frac{1}{2\pi}\left(\int_{EBZ} d^2k\ F_z - \oint_{\partial EBZ} d\mathbf{k}\cdot\mathbf{A}\right) \mathrm{mod}\ 2. \tag{1.54}$$

A modulo operation is imposed, since the second term is only gauge invariant modulo 2. This expression of w is different from the Chern number in a quantum Hall system, which only has the first term, and is an integral over a closed surface (the whole BZ).

Eq. (1.54) looks like the generalized **Gauss-Bonnet formula** for a 2D surface M with edge, in which the Berry curvature is replaced by the *Gaussian curvature* G, and the Berry connection is replace by the *geodesic curvature* k_g of the boundary,

$$\chi = \frac{1}{2\pi}\left(\int_M d^2r\ G - \oint_{\partial M} dr\ k_g\right). \tag{1.55}$$

For example, for a torus, $\chi = 0$, for a disk-like surface (which has a boundary), $\chi = 1$, and for a sphere, $\chi = 2$.

• Winding number of Zak phase

Recall that the Zak phase for a 1D Bloch state is

$$\gamma = \int_{-\pi}^{\pi} dk A(k). \tag{1.56}$$

The Chern number for a quantum Hall system is

$$C = \frac{1}{2\pi}\int_{BZ} d^2k F_z(\mathbf{k}). \tag{1.57}$$

One can choos the *parallel-transport gauge* (see Chap **??**),

$$\left\langle u_{k_xk_y}\left|\frac{\partial}{\partial k_y}\right|u_{k_xk_y}\right\rangle = 0, \tag{1.58}$$

so that $A_y(\mathbf{k}) = 0$. Then the phases of Bloch states are smooth inside the BZ, but are not continuous across upper (or lower) edges of the BZ.

With Stokes theorem, one gets

$$\begin{aligned} C &= \frac{1}{2\pi}\left(\int_{-\pi}^{\pi} dk_x A_x(k_x,\pi) - \int_{-\pi}^{\pi} dk_x A_x(k_x,-\pi)\right) \\ &= \frac{1}{2\pi}\int_{-\pi}^{\pi} dk_y \partial_{k_y}\gamma(k_y) \qquad (1.59) \\ &= \frac{1}{2\pi}\left[\tilde{\gamma}(\pi) - \gamma(-\pi)\right], \qquad (1.60) \end{aligned}$$

where $\gamma(k_y)$ is the Zak phase across the BZ with k_y fixed. We put a tilde on the first term to emphasize that its value depends on the history of the integration over k_y. In general, $\tilde{\gamma}(\pi) = \gamma(\pi) + 2\pi w$, $\gamma(\pi)$=$\gamma(-\pi)$ is single-valued, and w is the winding number of the mapping: $k_y \in [-\pi,\pi] \to \gamma(k_y)$. In the plot of $\gamma(k_y)$ (Fig. 5), w is the number of times the curve crosses $\gamma = 2\pi$ from below. Finally, we have $C = w$.

The Z_2 topological number ν, or ΔP_θ, is the difference of TR polarizations (Eq. (1.2)). When it is written in Zak phase ($qa = 1$), we have

$$\begin{aligned} \nu &= \frac{1}{2\pi}\left[\gamma_\theta(k_y=\pi) - \gamma_\theta(k_y=0)\right] \mathrm{mod}\ 2, \qquad (1.61) \\ \gamma_\theta &\equiv \gamma_+ - \gamma_-, \qquad (1.62) \end{aligned}$$

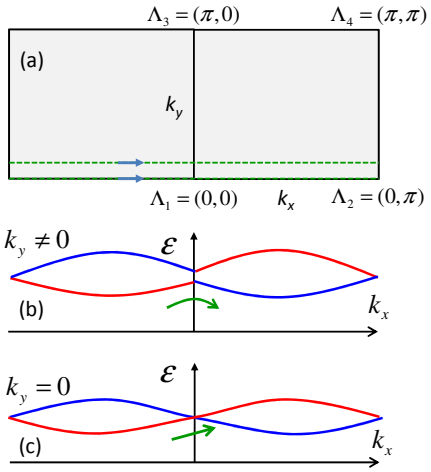

FIG. 6 Effective Brillouin zone (a). The energy dispersion of a Kramer pair along $k_y \neq 0$ (b) and $k_y = 0$ (c). To get the Zak phase $\gamma_\pm$, one needs to follow the green arrows when doing the integration.

where $\gamma_\pm$ are the Zak phases across $k_x \in [0, 2\pi]$ for the two eigenstates $u_{\mathbf{k}\pm}$. It is tempting to write the difference as

$$\nu = \frac{1}{2\pi}\int_0^\pi dk_y \partial_{k_y}\gamma_\theta(k_y), \tag{1.63}$$

as we have done for the quantum Hall state. However, this is wrong, since γ_θ is *not* continuous when k_y moves away from 0 or π, as shown in Fig. 6 (Grusdt *et al.*, 2014).

Instead, one writes,

$$\begin{aligned} 2\pi\nu &= \gamma_+(\pi) - \gamma_-(\pi) - [\gamma_+(0) - \gamma_-(0)] \qquad (1.64)\\ &= 2\left[\gamma_+(\pi) - \gamma_+(0)\right] - \sum_{\alpha=\pm}\left[\gamma_\alpha(\pi) - \gamma_\alpha(0)\right]. \end{aligned}$$

The second term, which relates to the charge polarization, *is* continuous throughout the BZ. Thus, it can be written as an integral over k_y. Furthermore, it is known that $\gamma_+ = \gamma_-$. Hence,

$$\begin{aligned} \gamma_c &\equiv \gamma_+ + \gamma_- = 2\gamma_+, \qquad (1.65)\\ 2\pi\nu &= \gamma_c(\pi) - \gamma_c(0) - \underbrace{\int_0^\pi dk_y \partial_{k_y}\gamma_c(k_y)}_{=\tilde{\gamma}_c(\pi)-\gamma_c(0)}. \qquad (1.66) \end{aligned}$$

The history-dependent phase $\tilde{\gamma}_c(\pi) = \gamma_c(\pi) + 2\pi w_c$, where w_c is the winding number of the mapping: $k_y \in [0, \pi] \to \gamma_c(k_y)$. Finally, we have $\nu = w_c \bmod 2$.

Note that, with the parallel-transport gauge,

$$\begin{aligned} &\int_{EBZ} d^2k\ F_z - \oint_{\partial EBZ} d\mathbf{k}\cdot\mathbf{A}\\ &= \int_0^\pi dk_y \partial_{k_y}\gamma_c(k_y) - [\gamma_c(\pi) - \gamma_c(0)]. \qquad (1.67) \end{aligned}$$

Thus, the winding number in Eq. (1.54) is the same as the winding number of the Zak phase.

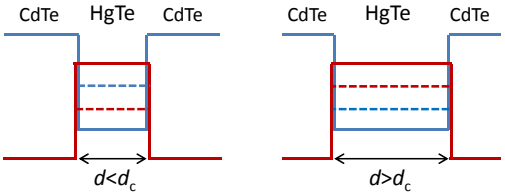

FIG. 7 HgTe is sandwiched between CdTe, forming a quantum well. The positions of the discrete energy levels in the QW depend on the width of the QW.

• Summary

So far we have learned that the Z_2 topological invariant ν can be calculated via,
1. The sign of pf $\mathsf{w}/\sqrt{\det \mathsf{w}}$ at TRIM (or, the parities of Bloch states at TRIM, *if* there is inversion symmetry).
2. The Gauss-Bonnet-like integral formula above.
In addition, ν can also be characterized by
3. The vorticity of the pfaffian of a sewing matrix m (see Prob. 2).
4. The axion angle of electromagnetic response (see Chap **??**).

Except for the parities in 1., none of these is easy to evaluate. For a crystal without inversion symmetry, one can deform it to one that has SIS and determine its ν by parities. This is a valid shortcut *if* the energy gap remains open during the process of deformation.

B. Bernevig-Hughes-Zhang model

There is a close relation between the Z_2 integer and the *band inversion* (*negative* energy gap) near the chemical potential. The first experimentally confirmed (2D) TI is made from semiconductor quantum well. Bulk HgTe has inverted band structure (due to spin-orbit coupling) near the Fermi energy. Unfortunately, it's a metal, not an insulator. Nevertheless, one can sandwitch it between CdTe (an ordinary insulator), forming a quantum well (QW) and opening an energy gap near the Fermi energy (see Fig. 7). When the HgTe layer is thick, the discrete QW energy levels remain inverted, similar to the bulk states. However, if the HgTe layer is thinner than a critical width d_c, then the electron (E1) and hole (H1) levels in the QW would switch positions. Therefore, one can check if the topology of the QW states (signified by the emergence of helical edge states) depends on the width of the QW (König *et al.*, 2007).

Typical semiconductor band structure near $k = 0$ is shown in Fig. 8. In a QW, the LH bands split off the HH bands, so in the simplified Bernevig-Hughes-Zhang (BHZ) model, only conduction band and one HH valence band are considered (each are two-fold degenerate). In order to investigate the parities of Bloch states at TRIM, we follow the lattice version of the BHZ model proposed by Fu and Kane, 2007 (also, see Nomura, 2016)

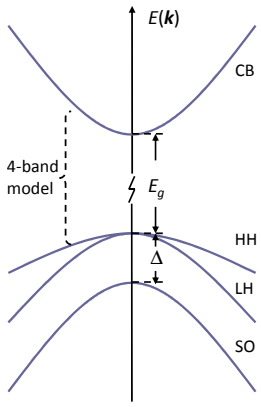

FIG. 8 Typical energy bands near the energy gap of a semiconductor, in which each line is two-fold degenerate. The conduction band is originated from the s-orbital. The valence band from the p-orbitals are composed of heavy-hole (HH) band, light-hole (LH) band, and spin-orbit split-off (SO) band.

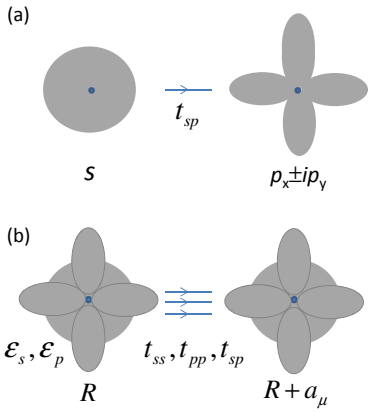

FIG. 9 (a) The hopping amplitude of an electron hopping from a s-orbital to the $p_x \pm ip_y$ orbitals of a nearest-neighbor atom is designated as t_{sp}. (b) Each atom has s-orbital and p-orbital, with energies ε_s and ε_p. An electron can hop between s-orbitals, between p-orbitals, or between an s-orbital and a p-orbital.

For an atom at site $\mathbf{R}$, four states are considered,

$$|s\uparrow\rangle, |s\downarrow\rangle, |p_x + ip_y\uparrow\rangle, |p_x - ip_y\downarrow\rangle. \tag{1.68}$$

Without ambiguity, one can write $|p_x + ip_y\uparrow\rangle$ and $|p_x - ip_y\downarrow\rangle$ simply as $|p\uparrow\rangle$ and $|p\downarrow\rangle$. They are the states with quantum numbers $m_j = 3/2$ and $m_j = -3/2$.

We consider only the electron hopping between nearest neighbors. The relevant parameters are on-site energies $\varepsilon_s, \varepsilon_p$, and hopping amplitudes t_{ss}, t_{pp}, and t_{sp} (and its complex conjugate t_{ps}), see Fig. 9. In a 2D square lattice, the vectors $\mathbf{R} + \mathbf{a}_\mu$ ($\mu = \pm x, \pm y$) point to the four nearest neighbors of $\mathbf{R}$. The tight-binding Hamiltonian is therefore given as,

$$\begin{aligned} H &= H_0 + H_1, \\ H_0 &= \sum_{\mathbf{R}\sigma=\pm} \left(\varepsilon_s |\mathbf{R}s\sigma\rangle\langle\mathbf{R}s\sigma| + \varepsilon_p |\mathbf{R}p\sigma\rangle\langle\mathbf{R}p\sigma|\right), \end{aligned} \tag{1.69}$$

and (given $t_{ps} = t_{sp}$)

$$\begin{aligned} H_1 = -\sum_{\mathbf{R}\sigma} \sum_{\mu=\pm x,\pm y} & \left(t_{ss} |\mathbf{R} + \mathbf{a}_\mu s\sigma\rangle\langle\mathbf{R}s\sigma| \right. \\ & - t_{pp} |\mathbf{R} + \mathbf{a}_\mu p\sigma\rangle\langle\mathbf{R}p\sigma| \\ & + e^{i\theta_\mu \sigma} t_{sp} |\mathbf{R} + \mathbf{a}_\mu s\sigma\rangle\langle\mathbf{R}p\sigma| \\ & \left. + e^{-i\theta_\mu \sigma} t_{sp} |\mathbf{R}p\sigma\rangle\langle\mathbf{R} + \mathbf{a}_\mu s\sigma| \right), \end{aligned} \tag{1.70}$$

where $\theta_\mu = \angle(\hat{x}, \mathbf{a}_\mu)$. That is, $\theta_x = 0, \theta_y = \pi/2, \theta_{-x} = \pi, \theta_{-y} = 3\pi/2$. Such a system has both TRS and SIS (details later).

Because of the lattice translation symmetry, the Hamiltonian can be diagonalized using the momentum basis. We therefore introduce the Fourier transformation (N is the total number of lattice sites),

$$|\mathbf{R}s\sigma\rangle = \frac{1}{\sqrt{N}} \sum_{\mathbf{k}} e^{i\mathbf{k}\cdot\mathbf{R}} |\mathbf{k}s\sigma\rangle, \tag{1.71}$$

$$|\mathbf{R}p\sigma\rangle = \frac{1}{\sqrt{N}} \sum_{\mathbf{k}} e^{i\mathbf{k}\cdot\mathbf{R}} |\mathbf{k}p\sigma\rangle, \tag{1.72}$$

and get (the lattice constant is set as one)

$$H = \sum_{\mathbf{k}} \left(\langle\mathbf{k}s\uparrow|, \langle\mathbf{k}s\downarrow|, \langle\mathbf{k}p\uparrow|, \langle\mathbf{k}p\downarrow|\right) \mathsf{H}(\mathbf{k}) \begin{pmatrix} |\mathbf{k}s\uparrow\rangle \\ |\mathbf{k}s\downarrow\rangle \\ |\mathbf{k}p\uparrow\rangle \\ |\mathbf{k}p\downarrow\rangle \end{pmatrix},$$

where

$$\begin{aligned} &\mathsf{H}(\mathbf{k}) \\ &= \begin{pmatrix} \varepsilon_s - 2t_{ss}(\cos k_x + \cos k_y) & 2t_{sp}(\sigma_z \sin k_y - i \sin k_x) \\ 2t_{sp}(\sigma_z \sin k_y + i \sin k_x) & \varepsilon_p + 2t_{pp}(\cos k_x + \cos k_y) \end{pmatrix}. \end{aligned} \tag{1.73}$$

Or,

$$\begin{aligned} \mathsf{H}(\mathbf{k}) &= \left[\frac{\varepsilon_s + \varepsilon_p}{2} - (t_{ss} - t_{pp})(\cos k_x + \cos k_y)\right] 1 \otimes 1 \\ &+ \left[\frac{\varepsilon_s - \varepsilon_p}{2} - (t_{ss} + t_{pp})(\cos k_x + \cos k_y)\right] \tau_z \otimes 1 \\ &+ 2t_{sp} \sin k_x \tau_y \otimes 1 + 2t_{sp} \sin k_y \tau_x \otimes \sigma_z. \end{aligned} \tag{1.74}$$

The Pauli matrices $\tau_{x,y,z}$ are for the orbital degree of freedom, and $\sigma_{x,y,z}$ are for the spin degree of freedom.

1. Time reversal and space inversion

Time reversal flips spin, but not orbital, therefore it acts only on the spin degree of freedom. The TR operator is thus,

$$\Theta = \begin{pmatrix} i\sigma_y K & 0 \\ 0 & i\sigma_y K \end{pmatrix} = 1 \otimes i\sigma_y K. \tag{1.75}$$

The s-orbital is even under space inversion, while the p-orbital is odd under SI. That is,

$$\Pi |\mathbf{k}s\sigma\rangle = |\mathbf{k}s\sigma\rangle, \tag{1.76}$$

$$\Pi |\mathbf{k}p\sigma\rangle = -|\mathbf{k}p\sigma\rangle. \tag{1.77}$$

Therefore,

$$\Pi = \begin{pmatrix} 1 & 0 \\ 0 & -1 \end{pmatrix} = \tau_z \otimes 1. \tag{1.78}$$

One can check that the Hamiltonian $\mathsf{H}(\mathbf{k})$ is indeed invariant under these two transformations,

$$\Theta \mathsf{H}(\mathbf{k}) \Theta^{-1} = \mathsf{H}(-\mathbf{k}), \tag{1.79}$$
$$\Pi \mathsf{H}(\mathbf{k}) \Pi^{-1} = \mathsf{H}(-\mathbf{k}). \tag{1.80}$$

2. Z_2 topological number

Since the BHZ model has SI symmetry, one can calculate the Z_2 topological number from the parities of the Bloch states at TRIM (see Fig. 1(b)). At a TRIM, the first line of Eq. 1.74 contributes a constant energy shift and can be ignored, and the third line is zero. Therefore,

$$\mathsf{H}(\Lambda_1) = \left[\frac{\varepsilon_s - \varepsilon_p}{2} - 2(t_{ss} + t_{pp})\right] \tau_z \otimes 1, \tag{1.81}$$
$$\mathsf{H}(\Lambda_2) = \left(\frac{\varepsilon_s - \varepsilon_p}{2}\right) \tau_z \otimes 1, \tag{1.82}$$
$$\mathsf{H}(\Lambda_3) = \left(\frac{\varepsilon_s - \varepsilon_p}{2}\right) \tau_z \otimes 1, \tag{1.83}$$
$$\mathsf{H}(\Lambda_4) = \left[\frac{\varepsilon_s - \varepsilon_p}{2} + 2(t_{ss} + t_{pp})\right] \tau_z \otimes 1. \tag{1.84}$$

Note that they are proportional to the parity operator,

$$\mathsf{H}(\Lambda_i) = g_i \Pi, \quad \Pi = \tau_z \otimes 1. \tag{1.85}$$

Hence, an energy eigenstate at Λ_i is also a parity eigenstate,

$$\Pi\psi = \zeta\psi \leftrightarrow \mathsf{H}(\Lambda_i)\psi = (g_i\zeta)\psi. \tag{1.86}$$

Let's assume $\varepsilon_s > \varepsilon_p$ in the following discussion. If $\varepsilon_s - \varepsilon_p > 4(t_{ss} + t_{pp}) > 0$, then the energies at Λ_1 are

$$\varepsilon_{1+} = +\left[\frac{\varepsilon_s - \varepsilon_p}{2} - 2(t_{ss} + t_{pp})\right], \tag{1.87}$$
$$\varepsilon_{1-} = -\left[\frac{\varepsilon_s - \varepsilon_p}{2} - 2(t_{ss} + t_{pp})\right]. \tag{1.88}$$

The degenerate eigenstates ψ_{1+} have even parity, while ψ_{1-} have odd parity. Only the state ψ_{1-} is filled, so $\delta(\Lambda_1) = -1$. Similarly, one can also get $\delta(\Lambda_2) = \delta(\Lambda_3) = \delta(\Lambda_4) = -1$. Therefore,

$$(-1)^\nu = 1, \text{ or } \nu = 0. \tag{1.89}$$

This is a trivial insulator.

On the other hand, if $\varepsilon_s - \varepsilon_p < 4(t_{ss} + t_{pp})$, then $\varepsilon_{1-} > \varepsilon_{1+}$. Due to the band inversion, now the states ψ_{1+} are filled instead. Therefore, $\delta(\Lambda_1) = 1$. The other three parities are not changed. As a result,

$$(-1)^\nu = -1, \text{ or } \nu = 1. \tag{1.90}$$

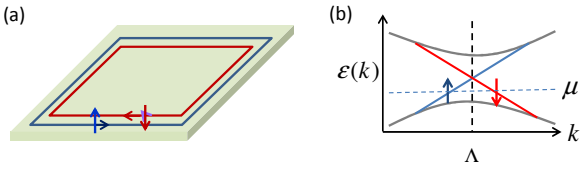

FIG. 10 (a) In real space, there is a helical edge state along the boundary of a 2D TI. (b) In momentum space, the energy dispersion curves of the edge states cross each other at a TRIM.

This is a topological insulator.

At the critical point, $\varepsilon_s - \varepsilon_p = 4(t_{ss} + t_{pp})$, the energy gap closes. The transition from the trivial phase to the topological phase is accompanied by an *inversion of energy bands*, when ε_+ and ε_- switch positions.

3. Orbital basis versus spin basis

Note that in Eq. 1.73, every 2×2 block of the Hamiltonian matrix is diagonal. In this case, it is possible to block-diagonal the 4×4 matrix by re-arranging the order of the basis,

$$|s\uparrow\rangle, |s\downarrow\rangle; |p\uparrow\rangle, |p\downarrow\rangle \tag{1.91}$$
$$\rightarrow |s\uparrow\rangle, |p\uparrow\rangle; |s\downarrow\rangle, |p\downarrow\rangle. \tag{1.92}$$

For convenience, we call the first choice the orbital basis, and the second the spin basis.

Under the spin basis, the Hamiltonian becomes (first switch the 2nd and the 3rd rows, then switch the 2nd and the 3rd columns of the matrix)

$$\mathsf{H}(\mathbf{k}) = \begin{pmatrix} \mathsf{h}(\mathbf{k}) & 0 \\ 0 & \mathsf{h}^*(-\mathbf{k}) \end{pmatrix}, \tag{1.93}$$

where

$$\begin{aligned} &\mathsf{h}(\mathbf{k}) \\ &= \begin{pmatrix} \varepsilon_s - 2t_{ss}(\cos k_x + \cos k_y) & 2t_{sp}(-i \sin k_x + \sin k_y) \\ 2t_{sp}(i \sin k_x + \sin k_y) & \varepsilon_p + 2t_{pp}(\cos k_x + \cos k_y) \end{pmatrix} \\ &= \varepsilon_0(\mathbf{k}) + 2t_{sp} \sin k_x \tau_y + 2t_{sp} \sin k_y \tau_x \\ &+ \left[\frac{\varepsilon_s - \varepsilon_p}{2} - (t_{ss} + t_{pp})(\cos k_x + \cos k_y)\right] \tau_z. \end{aligned} \tag{1.94}$$

Because of the block diagonalization, the up and down spins are explicitly decoupled.

Note that the TR and SI operators also are altered under the new basis. They now become

$$\Theta = i\sigma_y K \otimes 1, \ \Pi = 1 \otimes \tau_z. \tag{1.95}$$

4. QWZ model versus BHZ model

When written in the block-diagonal form, the Hamiltonian $\mathsf{h}(\mathbf{k})$ is similar to the QWZ model Hamiltonian for

the QAHE (see **??**). That is, the BHZ model is composed of two independent QWZ subsystems, $\mathsf{h}(\mathbf{k})$ and $\mathsf{h}^*(-\mathbf{k})$.

One can write

$$\mathsf{h}(\mathbf{k}) = \varepsilon_0(\mathbf{k}) + \mathbf{d}(\mathbf{k})\cdot\boldsymbol{\tau}, \tag{1.96}$$

then the Hall conductivity of the subsystem is,

$$\sigma_{xy} = -\frac{e^2}{h}\frac{1}{4\pi}\int_{BZ} d^2k \frac{1}{d^3}\mathbf{d}\cdot\frac{\partial\mathbf{d}}{\partial k_x}\times\frac{\partial\mathbf{d}}{\partial k_y}. \tag{1.97}$$

One can check that if $\varepsilon_s - \varepsilon_p > 4(t_{ss}+t_{pp})$, then the signs of $d_z(\mathbf{k})$ are all positive at the TRIM (analogous to Fig. **??**(a)). If $\varepsilon_s - \varepsilon_p < 4(t_{ss}+t_{pp})$, then $d_z(\Lambda_1)$ becomes negative, while the other three signs remain the same (see Fig. **??**(b)). According to the analysis of the QAHE in **??**, the first case has $\sigma_{xy}=0$, while the second case has $\sigma_{xy}=e^2/h$.

When the subsystem is in the QAH phase, according to the discussion in **??**, it has chiral edge states. Since this subsystem consists only of spin-up electrons (see Eq. 1.92), the edge-state electrons are spin-up. On the other hand, the conjugate subsystem $h^*(-\mathbf{k})$ has $\sigma_{xy}=-e^2/h$. Its edge electrons transport along the *opposite* direction and the spins are *down* (see Fig. 10(a)).

In momentum space, the energy dispersion of the edge state is linear in the small k-limit. One has positive slope (positive velocity), and the other has negative slope (negative velocity). Because of the Kramer degeneracy, these two dispersion curves have to cross each other at a TRIM (see Fig. 10(b)). This point degeneracy can be lifted *only if* the TRS is broken.

The topological phase of the BHZ model is called a 2D TI phase, aka a **quantum spin Hall** (QSH) phase. Its edge state, with one spin moving along one direction, and the opposite spin moving along the opposite direction, is called a **helical edge state**. It is robust in the sense that, even if there is a non-magnetic impurity $V_{imp}(\mathbf{r})$ blocking the way, the electron will not be back scattered since that requires a spin flip. Indeed, in the *Born approximation*, the transition amplitude for an edge state ψ_e being scattered to its time-reversed state $\theta\psi_e$ is proportional to the square of

$$\langle\psi_e|V_{imp}(\mathbf{r})|\theta\psi_e\rangle. \tag{1.98}$$

However, such a bracket is zero, as has been shown in Prob. 2 of Chap 1.

If there is a *magnetic impurity* that breaks TRS, then an electron could be backscattered, accompanied by a spin flip. Also, in the presence of *electron interaction*, there is a possibility that the edge is spontaneously magnetized. Should this happen, then the edge state is no longer protected by the TRS.

Some proposed materials for 2D topological insulator are 2D transition metal dichalcogenides (such as the 1T' form of WTe_2) (Cazalilla *et al.*, 2014, Qian *et al.*, 2014), and single-layer $ZrTe_5$ (Weng *et al.*, 2014, Li *et al.*, 2016). Several experimental reports can be found in, e.g., Fei *et al.*, 2017, Wu *et al.*, 2018, and Ugeda *et al.*, 2018.

Exercise

1. Start from the tight-binding Hamiltonian in Eqs. (1.69) and (1.70), switch to the momentum basis, and verify Eq. (1.73).

2. In addition to w, s, and v, a fourth type of sewing matrix is defined as

$$m_{\alpha\beta}(\mathbf{k}) = \langle u_{\mathbf{k}\alpha}|\Theta|u_{\mathbf{k}\beta}\rangle. \tag{1.99}$$

Consider the case with only one Kramer pair ($\alpha,\beta=\pm$):
a) Show that the matrix m is unitary and antisymmetric.
b) Show that

$$\mathsf{m}(-\mathbf{k}) = \mathsf{w}(\mathbf{k})\mathsf{m}^*(\mathbf{k})\mathsf{w}^T(\mathbf{k}). \tag{1.100}$$

c) With the help of the identity $\mathrm{pf}(\mathsf{BAB}^T) = (\det\mathsf{B})(\mathrm{pf}\ \mathsf{A})$, show that

$$\begin{aligned}\log[\det\mathsf{w}(\mathbf{k})] &= \log[\mathrm{pf}\ \mathsf{m}(-\mathbf{k})] - \log[\mathrm{pf}\ \mathsf{m}^*(\mathbf{k})]\\ &= \log[\mathrm{pf}\ \mathsf{m}(-\mathbf{k})] + \log[\mathrm{pf}\ \mathsf{m}(\mathbf{k})].\end{aligned} \tag{1.101}$$

d) Let Λ_x and Λ_y be 0 or π. Write $\mathrm{pf}\ \mathsf{m}(k_x,\Lambda_y)$ as $m(k_x)$; $\mathrm{pf}\ \mathsf{w}(k_x,\Lambda_y)$ as $w(k_x)$. Show that ($k_y=\Lambda_y$),

$$P_\theta = \frac{1}{2\pi i}\int_{-\pi}^{\pi} dk_x\ \partial_{k_x}\log m(k_x) + \frac{i}{\pi}\log\frac{m(\pi)}{m(0)}. \tag{1.102}$$

Note that $w(\Lambda_x) = m(\Lambda_x) = \pm 1$.
e) Finally, show that

$$\begin{aligned}\Delta P_\theta &\equiv P_\theta(k_y=\pi) - P_\theta(k_y=0)\\ &= \frac{1}{2\pi i}\oint_{\partial EBZ} d\mathbf{k}\cdot\partial_{\mathbf{k}}\log[\mathrm{pf}\ \mathsf{m}(\mathbf{k})] \mod 2\end{aligned} \tag{1.103}$$

where $EBZ = [-\pi,\pi]\times[0,\pi]$ is the upper half of the BZ. That is, the Z_2 topological invariant is the total vorticity of the zeros of $\mathrm{pf}[\mathsf{m}(\mathbf{k})]$ in the effective BZ. For more details, see Fu and Kane, 2006 and Sec. 4.5 of Fruchart and Carpentier, 2013.

References

Cazalilla, M. A., H. Ochoa, and F. Guinea, 2014, Phys. Rev. Lett. **113**, 077201.

Fei, Z., T. Palomaki, S. Wu, W. Zhao, X. Cai, B. Sun, P. Nguyen, J. Finney, X. Xu, and D. H. Cobden, 2017, Nature Physics **13**, 677.

Fruchart, M., and D. Carpentier, 2013, Comptes Rendus Physique **14**, 779 .

Fu, L., and C. L. Kane, 2006, Phys. Rev. B **74**, 195312.

Fu, L., and C. L. Kane, 2007, Phys. Rev. B **76**, 045302.

Grusdt, F., D. Abanin, and E. Demler, 2014, Phys. Rev. A **89**, 043621.

König, M., S. Wiedmann, C. Brüne, A. Roth, H. Buhmann, L. W. Molenkamp, X.-L. Qi, and S.-C. Zhang, 2007, Science **318**(5851), 766.

Li, X.-B., W.-K. Huang, Y.-Y. Lv, K.-W. Zhang, C.-L. Yang, B.-B. Zhang, Y. B. Chen, S.-H. Yao, J. Zhou, M.-H. Lu, L. Sheng, S.-C. Li, *et al.*, 2016, Phys. Rev. Lett. **116**, 176803.

Moore, J. E., and L. Balents, 2007, Phys. Rev. B **75**, 121306.

Nomura, K., 2013, Fundamental theory of topological insulator, unpublished, written in Japanese.

Nomura, K., 2016, *Topological insulator and superconductor* (Maruzen Publishing Co.), in Japanese.

Qian, X., J. Liu, L. Fu, and J. Li, 2014, Science **346**(6215), 1344.

Ugeda, M. M., A. Pulkin, S. Tang, H. Ryu, Q. Wu, Y. Zhang, D. Wong, Z. Pedramrazi, A. Martín-Recio, Y. Chen, F. Wang, Z.-X. Shen, *et al.*, 2018, Nature Communications **9**, 3401.

Weng, H., X. Dai, and Z. Fang, 2014, Phys. Rev. X **4**, 011002.

Wu, S., V. Fatemi, Q. D. Gibson, K. Watanabe, T. Taniguchi, R. J. Cava, and P. Jarillo-Herrero, 2018, Science **359**(6371), 76.